Arrival-time fluctuations of coherent reflections from surface gravity water waves

Mohsen Badiey,[a] Justin Eickmeier, and Aijun Song
College of Earth, Ocean, and Environment, University of Delaware, 107 Robinson Hall, Newark, Delaware 19716
badiey@udel.edu, jeickmei@udel.edu, ajsong@udel.edu

Abstract: Arrival time fluctuations of coherent reflections from surface gravity waves are examined. A two-dimensional ray model with an evolving rough sea surface is used to explain the mechanism and formation of the deterministic striation patterns due to the surface reflection. Arrival time predictions from the ray model match qualitatively well with the measurements from bidirectional acoustic transmissions in a water depth of 100 m.

PACS numbers: 43.30.Hw, 43.30.Re, 43.30.Es [JL]
Date Received: December 19, 2013 **Date Accepted:** March 19, 2014

1. Introduction

Surface gravity waves can have significant effects on high frequency (7 to 13 kHz) acoustic wave reflection, scattering, and propagation. Here, the particular focus is on coherent reflections from the dynamic upper boundary. This problem has been of interest in the underwater acoustics community for several years. A comprehensive review of scattering and reflection of sound waves at the ocean surface was given in 1970, when acoustic interactions with a rough surface were defined as functions of time, acoustic frequency, and geometry.[1]

In the following decades, several theoretical and experimental studies were conducted in high frequency acoustic signal propagation and scattering in shallow water regions, where the effects of the moving sea surface can be important.[2–4] In the late 1990s assessment of the channel impulse response functions in frequency ranges of 1 to 25 kHz related to temporal changes of the water column and the sea surface gained attention. This led to observation and understanding of some deterministic features of time evolving channel impulse response functions.[5,6] In 2004, coherent returns from the sea surface were reported in a very shallow waveguide (6 m depth)[7] and strong, fast-fluctuating acoustic focusing, referred to as a butterfly pattern, were explained by the formation of caustics due to the shoaling surface waves. Later, theoretical results from wavefront modeling, along with a tank experiment at the acoustic frequency of 200 kHz, showed that interference patterns occur as a result of multiple surface-reflected eigenrays from neighboring wave crests.[8] Most recently, an experiment conducted in a water depth of 15 m demonstrated highly transient surface reflection arrivals resulting from deterministic forward surface reflections.[9]

During the summer of 2011, an experiment was performed (referred to as the KAM11 experiment) in a water depth of 100 m near the Kauai Island, Hawaii, where reciprocal transmissions from two bottom-mounted transducers were performed.[10] Strong striation patterns with extended delay in surface bounced arrivals were shown. These patterns were modeled using a two-dimensional (2D) parabolic equation model.[10] In this paper, we present the driving mechanism behind the formation of striation patterns using a ray model combined with a time evolving sea surface. We examine the corresponding effects of surface wave spectrum spread and high frequency

[a]Author to whom correspondence should be addressed.

surface waves. This problem is inherently three-dimensional; however, for this study we limit our discussions to the 2D plane, following the methodology used in Ref. 10, where qualitative agreement between the data and model output was obtained. This paper is organized as follows: Section 2 presents the acoustic and surface wave observations from the KAM11 experiment. Section 3 explains the mechanism of the coherent reflection using the BELLHOP ray model[11] with moving surfaces. This explanation is extended in Sec. 4 to include the ray model results under a measured surface wave spectrum and to show the data model comparison. Section 5 provides a summary of this work.

2. KAM11 experiment

The KAM11 experiment was conducted during the summer of 2011 in a 100 m deep, shallow water region near Kauai Island, Hawaii.[10] Two seafloor tripod transceiver systems configured with an 8-element hydrophone array and top mounted transducer were deployed 1 km apart at STA05 and STA07 as shown in Fig. 1(a), on July 10th and 11th. Repeated 40 s chirp sequences (bandwidth of 7 to 13 kHz and duration of 48 ms for a single chirp signal) were sent on a 4-min schedule with a 2-min offset from the two tripods. A monitoring hydrophone was deployed at a depth of 25 m from the bow of the *R/V Kilo Moana*, which held station by a dynamic positioning system approximately midway between the two tripods [Fig. 1(a)]. A 16-element thermistor string and a Waverider buoy collected environmental data. Here the measurements collected on July 10, 2011 23:52-54 UTC are analyzed. Figures 1(b) and 1(c) show power spectral density (S_f) for surface wave spectra and sound speed profiles, respectively, throughout the tripod deployment. The dominant wave direction was about 42° to 45° from the Northeast, consistent with the wave direction over the frequencies of 0.1 to 0.3 Hz, where the main wave energy was concentrated.

Figure 1(d) shows the measured impulse responses between the STA05 source and the monitoring hydrophone. Figure 1(e) shows the arrival patterns from the reciprocal STA07 transmission. The acoustic measurements in both subplots show coherent reflections from moving surface waves. Different parts of the ocean surface can generate strong, coherent reflections, which arrive at the receiving monitoring hydrophone

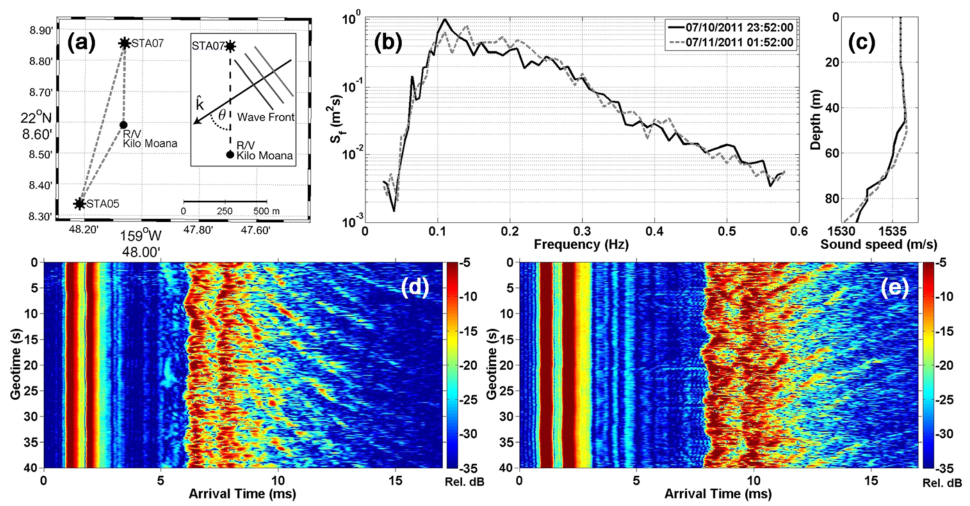

Fig. 1. (Color online) KAM11 observations. (a) Experimental geometry showing the angle between the surface wave propagation and the acoustic track. The average angles $\theta = 42°$ for the acoustic track between STA07 and the monitoring hydrophone and $\theta = 12°$ for the STA05 track. (b) Measured wave spectrums and (c) sound speed profiles for two different geotimes. (d) Measured intensity impulse response from STA05 to the monitoring hydrophone. (e) Measured intensity impulse responses from STA07 to the monitoring hydrophone.

at varying arrival times (relative to range of the surface reflection from the receiver). These short-time surface-interacting paths cover an extended span in arrival time. When the ocean surface moves, some of the coherent surface returns show varying delay over time, giving a striation pattern. The striation pattern has a strong directionality, which relates to the angle between the acoustic track and the relative direction of surface wave front **k** [Fig. 1(a) inset]. Based on examination of surface returns, the moving surface generated Doppler shifts in the 0.25 to 2 Hz range. This amount of Doppler shift did not impact the pulse compression process of the chirp sequences.

We define θ as the angle between the acoustic track and the dominant surface wave train such that when the surface waves propagate parallel to the acoustic track, the angle is $0°$, that is, $\theta = 0°$. When $\theta = 90°$, the acoustic track and surface wave propagation are perpendicular. Increasing θ leads to a longer apparent surface wave wavelength, λ_s, projected in the 2D plane, which encompasses the acoustic source and receiver. The relationship is given by $\lambda_s = \lambda/\cos\theta$, where λ is the true surface wave wavelength. The average angles are $\theta = 42°$ for the acoustic track between STA07 and the monitoring hydrophone and $\theta = 12°$ for the STA05 track during the measurement period considered (Fig. 1).

3. Mechanism of the coherent reflections

We use the BELLHOP ray model, combined with moving sea surface inputs, to study the mechanism of the observed coherent reflections. When the surface progresses over time, the snapshots of the moving surface are fed to the BELLHOP model. The ray model calculates the acoustic rays under each surface snapshot. With multiple successive runs, the acoustic model generates time-varying acoustic arrivals.

Figure 2(a) shows the ray diagram under a snapshot of a moving sinusoidal surface where the source/receiver geometry matches the STA05 to monitoring hydrophone track. The properties of the sinusoidal surface are taken from the measured surface wave spectrum in Fig. 2(d), which has a peak amplitude at 0.11 Hz. The corresponding wavelength is 129 m and the significant wave height is 1.5 m. Three segments of the surface, one at a wave crest and two around the neighboring troughs, reflect the

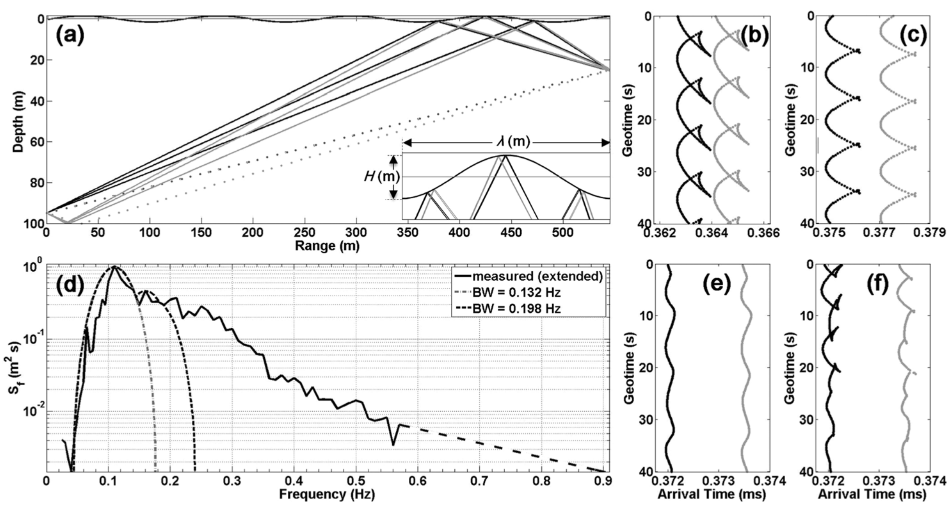

Fig. 2. Coherent reflections from sinusoidal and random surfaces. (a) BELLHOP ray trace diagram. (b) Arrival time patterns of the surface returns under a moving sinusoid surface wave. Surface wave frequency, wavelength, and height are chosen as 0.11 Hz, 129 m, and 1.5 m, respectively, for $\theta = 0°$. (c) Similar to (b), except $\theta = 50°$. (d) Measured surface wave spectrum with high frequency extension. Arrival time patterns of the surface returns for wave bandwidths of 0.132 Hz (e) and 0.198 Hz (f).

acoustic rays to the receiver, generating three micro-paths for the surface eigenrays (black) in Fig. 2(a) inset. Due to the close proximity of the source to the seafloor, the same phenomenon generates the surface-bottom interacting paths (gray).

When the surface wave moves slightly, the reflections from three surface patches can still reach the receiver as coherent arrivals. The arrival patterns for the surface and bottom eigenrays are shown in Fig. 2(b) under the moving sinusoid surface for 40 s. We note that the ray arrival pattern is closely related to the butterfly structure that was previously reported in a very shallow water waveguide.[6]

Due to the source-receiver geometry, the butterfly shape resulting from a sinusoidal wave is not symmetric. Rather, it is skewed as shown in Fig. 2(b) and arrival time delay in the butterfly pattern increases with geotime. When the direction of surface wave propagation is reversed in the sinusoidal surface simulation, the arrival time delay in the butterfly pattern decreases with geotime progression. This is similar to the observed data [see Figs. 1(d) and 1(e)]. When source and receiver are at the same depth, a symmetrical butterfly is generated. Ray simulations show that variation of the water column sound speed profile in this experimental data has limited impacts on the butterfly shape and its formation.

We define $\beta = H/\lambda_s$ as the ratio of the significant wave height H to the surface wavelength λ_s along the acoustic track in the 2D acoustic propagation plane. The ratio β is important to the formation of the caustics under the moving surface. For a given range and geometry, a threshold ratio exists above which the butterfly shape will form in the arrival pattern. A larger value of β is more likely to generate the butterfly shape since it corresponds to a steep surface wave shape. We note that the angle between the surface wave train relative to the acoustic path becomes important as it changes the projected surface wavelength λ_s. Computer simulations reveal that sinusoidal surface waves with parameters $\theta = 50°$ and $\lambda_s = 129$ m narrowly allow butterfly pattern formation in Fig. 2(c) for a significant surface wave height of 1.5 m. For this geometry, the threshold for "butterfly" formation is $\beta > 0.007$. This corresponds to a projected wavelength of 215 m and significant wave height of 1.5 m. The threshold for butterfly formation was obtained from computer simulations, specifically the BELLHOP simulations over the sinusoidal wave surfaces. If the values of λ or H are modified such that $\beta < 0.007$, the wave steepness is no longer sufficient to form folded wavefront arrivals.

To reproduce the surface effects observed in the experiment, we used an evolving linear sea surface model for inputs to BELLHOP.[12] We note that a single-frequency sinusoidal surface wave cannot create the extended delays shown in the data [Figs. 1(d) and 1(e)]. The extended delays are only created under surface waves with spread spectra. The smooth arrival pattern without caustics in Fig. 2(e) results from running BELLHOP with a narrow spectrum with bandwidth = 0.132 Hz in Fig. 2(d). Inclusion of some high frequency components of the surface wave can increase the chance for the caustics. This is shown by extending the narrow spectrum by 50% to a bandwidth of 0.198 Hz. The resultant arrival time pattern for the surface path is shown in Fig. 2(f), where the butterfly formation appears at the beginning and fades out after 20 s. The disappearance of the caustics is caused by the smaller wave crests passing through the acoustic track.

4. Coherent reflection under a linear surface wave

A data-model comparison is performed by running BELLHOP based on the experimental setup and using the measured sound speed profile and surface wave spectrum on July 10, 2011 23:52-54 UTC, a different period than previously examined.[10] The surface wave spectrum was extended to 2 Hz and rolls off in a manner $\sim\omega^{-5}$ [dashed line starting from 0.6 Hz in Fig. 2(d)]. The moving surface was simulated based on the extended wave spectrum, augmented with a random phase. Therefore, the data-model comparison shown in this section is a statistical one. The surface simulation used the directional information over all the wave frequency components.

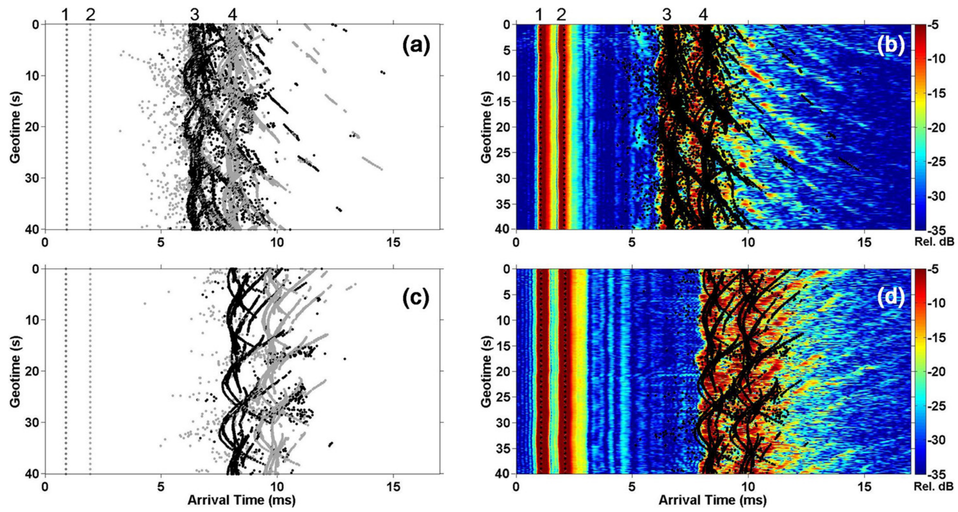

Fig. 3. (Color online) Data-model comparison for arrival time patterns. (a) Ray results for the STA05 source. (b) Overlay of the model results on measured impulse response for the STA05 source. (c) Ray results for the STA07 source. (d) Overlay of the model results on measured impulse response for the STA07 source.

Figure 3 shows the data-model comparison results. Figure 3(a) shows the BELLHOP modeling results for the STA05 to monitoring hydrophone path, while Fig. 3(b) displays this result overlaid on the measured impulse response for this acoustic track. Figure 3(b) shows notable agreements between the measurements and modeled results. The direct and bottom paths are evident in the comparison (both data and model outputs). Multiple features of surface reflections are predicted by the ray model. First, the early surface reflection arrivals from the measurements show undulations when the sea surface moves up-and-down. This is reflected in the model outputs. Second, coherent reflection patterns or “striations” with extended delay are modeled by the ray model. The trend in impulse response measurements is closely matched by the overlaid BELLHOP results in the 6 to 10 ms arrival time range. Third, both data and model outputs show that the surface reflections extend into the 10 to 15 ms range in arrival-time intermittently for the STA05 source. These late surface returns share the directionality of the earlier reflection patterns and are closely approximated by the BELLHOP outputs.

Figures 3(c) and 3(d) share much of the above similarity in direct, bottom, and initial surface paths. However, the transmission direction is reversed and the range is shorter. It is 460 m for the STA07 source transmissions, compared with 570 m for the STA05 sequences. As a result, the directionality of the striations is reversed, showing decreasing arrival time delays with advancing geotime. In the 8 to 12 ms range, there is good agreement between measured striation directionality and BELLHOP results. It is noted that extension of coherent surface wave reflections in the arrival time was dependent on the wave spectrum spread.

5. Conclusion

In this Letter, we have analyzed acoustic bidirectional transmissions during the KAM11 experiment, with a focus on arrival time fluctuations of coherent reflections from the surface gravity waves. A 2D ray model with an evolving rough sea surface has been used to explain the mechanism and formation of the deterministic striation patterns. With a moving linear surface wave generated from measured surface spectrum, the 2D ray model can provide qualitative matching results for the arrival time fluctuating of the surface returns.

Acknowledgments

This research was supported by the Office of Naval Research (ONR) Code 322OA through Grant No. N00014-13-1-0306. The authors wish to thank all participants of the KAM11 experiment.

References and links

[1] L. Fortuin, "Survey of literature on reflection and scattering of sound waves at the sea surface," J. Acoust. Soc. Am. **47**, 1209–1228 (1970).
[2] E. I. Thorsos, "Acoustic scattering from a 'Pierson-Moskowitz' sea surface," J. Acoust. Soc. Am. **88**, 335–349 (1990).
[3] K. L. Williams, J. S. Stroud, and P. L. Marston, "High-frequency forward scattering from Gaussian spectrum, pressure release, corrugated surfaces. I. Catastrophe theory modeling," J. Acoust. Soc. Am. **96**, 1687–1702 (1994).
[4] P. H. Dahl, "On the spatial coherence and angular spreading of sound forward scattered from the sea surface: Measurements and interpretive model," J. Acoust. Soc. Am. **100**, 748–758 (1996).
[5] M. Badiey, J. A. Simmen, and S. Forsythe, "Frequency dependence of broadband propagation in coastal regions," J. Acoust. Soc. Am. **101**, 3361–3370 (1997).
[6] M. Badiey, Y. Mu, J. A. Simmen, and S. E. Forsythe, "Signal variability in shallow-water sound channels," IEEE J. Ocean. Eng. **25**(4), 492–500 (2000).
[7] J. C. Preisig and G. B. Deane, "Surface wave focusing and acoustic communications in the surf zone," J. Acoust. Soc. Am. **116**, 2067–2080 (2004).
[8] C. T. Tindle, G. B. Deane, and J. C. Preisig, "Reflection of underwater sound from surface waves," J. Acoust. Soc. Am. **125**, 66–72 (2009).
[9] G. B. Deane, J. C. Preisig, C. T. Tindle, A. Lavery, and M. D. Stokes, "Deterministic forward scatter from surface gravity waves," J. Acoust. Soc. Am. **132**, 3673–3686 (2012).
[10] M. Badiey, A. Song, and K. B. Smith, "Coherent reflection from surface gravity water waves during reciprocal acoustic transmissions," J. Acoust. Soc. Am. **132**, EL290–EL295 (2012).
[11] M. B. Porter and H. P. Bucker, "Gaussian beam tracing for computing ocean acoustic fields," J. Acoust. Soc. Am. **82**, 1349–1359 (1987).
[12] E. A. Karjadi, M. Badiey, J. T. Kirby, and C. Bayindir, "Effects of surface gravity waves on high-frequency propagation in shallow water," IEEE J. Ocean. Eng. **37**, 112–121 (2012).